Ninth International Conference on Computational Fluid Dynamics (ICCFD9), Istanbul, Turkey, July 11-15, 2016

ICCFD9-0182

Multilevel ADER Scheme For Computational Aeroacoustics

S. M. Joshi* & A. Chatterjee

Department of Aerospace Engineering
Indian Institute of Technology, Bombay
Mumbai 400076, India

Abstract: The versatile ADER scheme [1] is cast in a multilevel framework (ML-ADER) for fast solution of linear hyperbolic PDEs. The solution is cycled through spatial operators of decreasing accuracy while retaining highest-order accuracy by the use of a forcing function. Results are obtained for benchmark problems in computational aeroacoustics at a much reduced computational cost.

Keywords: ADER, Multi-Level, Linear PDEs, Computational Aeroacoustics.

1 Introduction

Linear hyperbolic PDEs govern behaviour of linear traveling waves in aeroacoustics and electromagnetics. Numerical schemes used to solve such systems are required to preserve phase and amplitude over large computational domain and long simulation time. This requires schemes with very low dispersion and dissipation errors. Dissipation errors can be reduced by the use of a higher-order method. Dispersion errors in turn can be reduced either by using a higher-order scheme or by a numerical scheme optimized for minimum errors over a limited range of wavenumbers. Cunha and Redonnet [2] recently showed that spectrally optimized schemes may not be suitable for well-resolved waves since they can result in overall greater error compared to uniformly higher-order accurate schemes. Uniformly higher-order schemes may prove to be more effective in reducing dispersion and dissipation errors, especially in the case of well resolved waves.

However, a major drawback of higher-order schemes, is the high computational cost per-grid point. The use of coarser grids resulting from a more relaxed Points-Per-Wavelength (PPW) criteria in case of higher-order schemes results in reduced number of computations compared to lower-order schemes. On the other hand, higher cost per-grid point may actually result in an overall increase in computational cost for higher-order schemes. Traditionally, Multi-Grid (MG) methods have been effectively used for accelerating convergence of iterative solvers resulting from numerical discretization of PDEs [3]. In the MG method, the error is progressively smoothened out by cycling through a hierarchy of successively coarser grids (h-MG) or through a succession of lower-order spatial reconstruction (p-MG) or a combination of both. However, MG methods based on smoothing properties of iterative solvers are best suited for driving numerical solution of boundary value problems to an accelerated steady state [3] and may not be appropriate for the time accurate solution of travelling waves governed by hyperbolic PDEs.

A Multi-Level (ML) method was developed in Ref.[4] for fast computation of travelling linear waves governed by linear hyperbolic PDEs. In this method, higher-order accuracy is inexpensively and exactly maintained at coarser approximations in the advection process which characterizes time-dependant linear wave propagation. This is achieved by cycling the solution through successively lower orders of reconstruction in the solution process. The relative truncation error (τ) between two consecutive levels is used as a forcing function to enforce highest-order accuracy at lower levels while retaining time accuracy. The ML method in a Finite-Volume Essentially-Non-Oscillatory (ENO) framework was successfully implemented for solving

*email: smjoshi@aero.iitb.ac.in

problems in electromagnetics and aeroacoustics [4, 5]. In this paper, we extend application of the ML algorithm to the versatile ADER (Arbitrary higher order DERivatives) scheme (ML-ADER).

The ADER scheme is especially compatible with the ML framework because of its high spatial and temporal accuracy, along with flexibility of reconstruction [1]. In the ML-ADER framework, highest-order accuracy is uniformly maintained when cycling the solution through successive lower-order approximations while solving the linear hyperbolic PDE. In this study, sawtooth and frozen-τ variants from MG methods are implemented for the ML-ADER method. In the sawtooth version, a single time-step is executed at all including lowest level ($\nu = 1$), whereas in the frozen-τ variant, multiple time-steps are performed at the lowest level ($\nu > 1$) while maintaining highest-order accuracy, thereby further reducing computational cost. In addition, error analysis for the ML-ADER method, along with saving in computing cost due to implementation of the multilevel framework, is presented.

2 ML-ADER Method

2.1 Multilevel Method

Consider a system of hyperbolic Partial Differential Equations (PDEs) in 2D,

$$\mathbf{U}_t + \mathbf{F}_x + \mathbf{G}_y = 0 \tag{1}$$

where, $\mathbf{U} = [u_1, u_2, ..., u_n]^T$ is a vector of conserved variables and $\mathbf{F} = [f_1(\mathbf{U}), f_2(\mathbf{U}), f_3(\mathbf{U}), ..., f_n(\mathbf{U})]^T$, $\mathbf{G} = [g_1(\mathbf{U}), g_2(\mathbf{U}), g_3(\mathbf{U}), ..., g_n(\mathbf{U})]^T$ are the flux vectors in x, y directions respectively. The semi-discrete formulation of the given hyperbolic PDE resulting from the finite volume approximation is given as,

$$\left.\frac{d\mathbf{U}_i}{dt}\right|_n = \mathcal{R}_p^n = \left.\frac{-1}{V_i}\sum_{j=1}^{N} \mathbf{F}_j^* . \hat{\mathbf{n}}_j l_j\right|_n \tag{2}$$

Where, $\mathbf{F}^*$ is the numerical flux $[\mathbf{F}, \mathbf{G}]$ at j^{th} face of i^{th} Finite-Volume (FV) cell. l_j is the length of the j^{th} face and $\hat{\mathbf{n}}_j$ is a unit normal $[n_x, n_y]$ to the j^{th} face. p is the order of the interpolation-polynomial used for data reconstruction. For $p = 0$, this will yield traditional first-order finite volume scheme. n indicates the time level at which computations are performed. Thus, $\mathcal{R}_p^n$ is the p^{th}-order flux-residual in the i^{th} finite volume at time level n.

In the conventional finite volume numerical schemes, equation(2) is integrated numerically to advance the solution in time. At each time-step, a p^{th} order polynomial is used for data reconstruction. This results in uniformly p^{th}-order accurate single-level FV scheme. In the ML method however, the solution is cycled through successively coarser approximations. Thus, after computing $\mathcal{R}_P^{(n-1)}$, computations at level n are performed using $(p-1)^{th}$ order polynomial. To retain higher-order accuracy at coarser approximations, the relative truncation error between $R_p^{(n-1)}$ and $R_{p-1}^{(n-1)}$ is used as the forcing function. The relative truncation error (τ) between two consecutive orders of reconstruction is defined as,

$$\tau_{p-1}^n = \mathcal{R}_p^{(n-1)} - \mathcal{R}_{p-1}^{(n-1)} + \tau_p^{(n-1)} \tag{3}$$

At the highest level ($p = m$), the forcing function $\tau_m = 0$. The modified residual at time level n is then defined as,

$$\hat{\mathcal{R}}_{p-1}^n = \mathcal{R}_{p-1}^n + \tau_{p-1}^n$$

The resultant ODE is given as,

$$\frac{d\mathbf{U}_i}{dt} = \hat{\mathcal{R}}_{p-1} \tag{4}$$

At time level n, equation(4) using the modified residual $\hat{R}_{p-1}$ is integrated numerically to advance the solution.

The modified residual $\hat{R}_{p-1} = R_{p-1} + \tau_{p-1}$ using a $(p-1)^{th}$-order reconstruction in a standard finite volume formulation turns out to be p^{th}-order accurate under the condition of local linearity [5]. Further it can be argued that at all levels of approximation, highest-order accuracy can be retained by successive

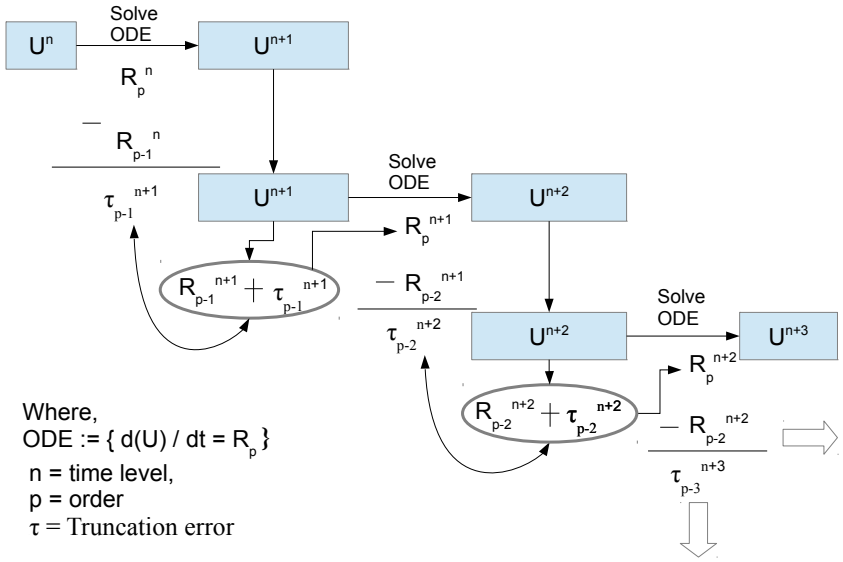

Figure 1: ML Algorithm: Addition of the Truncation Error as the Forcing Function

addition of τ as a forcing function to lower-order residuals. This process is illustrated in Fig.1. Since the computational cost of polynomial reconstruction is significantly lower for lower orders, cycling in lower-order accurate approximations reduces overall computational cost.

2.2 ML-ADER Implementation

The ADER scheme (**A**rbitrary high order scheme, which utilises the hyperbolic Riemann problem for the advection of the higher order **DER**ivatives) is based on the MGRP (Modified Generalized Riemann Problem) scheme of Toro [6]; which in turn is a simplification of the Generalized Riemann Problem (GRP) scheme of Ben-Artzi and Falcovitz [7]. Schwartzkopff and Toro further developed the ADER scheme for linear systems [1, 8]. Application of the ADER scheme to non-linear hyperbolic problems, as well as 3D generalization were carried out by Titarev and Toro [9, 10, 11]. ADER schemes are found to be especially suitable for wave propagation because of dampening of the dispersive modes thereby preserving wave phase and amplitude [1]. A brief description of the ADER method is presented in the following section.

A Riemann problem arising from piecewise polynomial data is known as the Derivative Riemann Problem (DRP) [12]. Solution of the DRP yields the state variable, as well as higher-order spatial derivatives of the state variable at cell interfaces. Corresponding time-derivatives can be obtained using the Lax-Wendroff procedure which links time-derivatives to the spatial derivatives. Time-derivatives of the state variable at interfaces in turn can be used for the Taylor series approximation of time-evolution of the state variable. Thus, in the ADER scheme, higher-order approximation to the state variable along the t-axis is obtained by combining higher-order spatial reconstruction and finding solution of the DRP at cell interfaces[12]. The (K^{th}-order) Taylor series expansion of the state variable is written as, (note, $\frac{\partial}{\partial t}$ is written as ∂_t and $\frac{\partial}{\partial x}$ as ∂_x)

$$\mathbf{U}^{ADER}(\tau) = \underbrace{\mathbf{U}_{face}(0_+)}_{1} + \underbrace{\sum_{k=1}^{K} \left[\partial_t^{(k)} \mathbf{U}_{face}(0_+)\right] \frac{\tau^k}{k!}}_{2} \tag{5}$$

where, the first term on the right hand side is the solution of the conventional Riemann problem based on the discontinuity in the state variable at cell interfaces (Godunov state). The second term is obtained by first converting the time derivatives into spatial derivatives using the Lax-Wendroff procedure and then solving $K-1$ DRPs at the cell interface for obtaining the space derivatives at the interface. For a 1D linear

system, k^{th} DRP is given by,

$$\partial_t(\partial_x^{(k)}\mathbf{U}) + \mathbf{A}_{face}\partial_x(\partial_x^{(k)}\mathbf{U}) = \mathbf{0} \tag{6}$$

where,

$$\partial_x^{(k)}\mathbf{U}(x,0) = \begin{cases} \partial_x^{(k)}\mathbf{U_L}(0) & \text{if} \quad x < 0, \\ \partial_x^{(k)}\mathbf{U_R}(0) & \text{if} \quad x > 0. \end{cases}$$

For linear systems, the coefficient matrix $\mathbf{A}_{face}$ is constant. The direction of characteristic waves at the interface is found out only once during computation of the Godunov state. Same information can be used when solving for higher-order derivatives. Further details regarding the ADER procedure and 2D implementation can be found in Ref.[1]. Once the state variable value at interfaces is known, the numerical flux can be computed as $\mathbf{F}^{ADER} = \mathbf{A}_{face}\mathbf{U}^{ADER}$, where $\mathbf{A}_{face}$ is the constant coefficient matrix and $\mathbf{U}^{ADER}$ is the state variable vector at the cell interface obtained by solving equation (5). Then the evolution equation (2) can be written as,

$$\frac{d\mathbf{U}_i}{dt} = \mathcal{R}_p^{ADER} = \frac{-1}{V_i}\sum_{j=1}^{N}\mathbf{F}_j^{ADER}.\hat{\mathbf{n}}_j l_j$$

where, $\mathbf{F}^{ADER}$ is the numerical flux obtained with the ADER scheme. This in turn can be solved using the Euler time-stepping given as,

$$\mathbf{U}_i^{n+1} = \mathbf{U}_i^n + \Delta t\mathcal{R}_p^{ADER} \tag{7}$$

where, Δt is the time-step governed by the CFL condition. The numerical scheme given by equation (7) is higher-order accurate both in space and time as a result of spatial-temporal coupling in the Lax-Wendroff procedure.

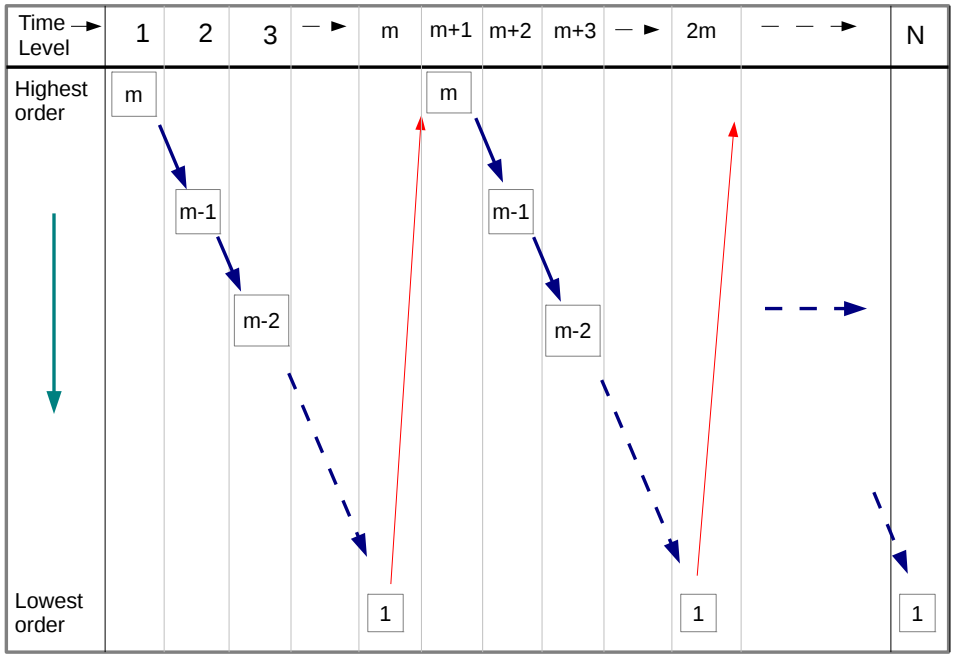

Figure 2: ML Algorithm: Cycling the Solution Through Successively Coarser Approximations

The ML-ADER method can be summarized as,

- Define number of levels in each cycle (m) and total number of cycles (N)

- At the highest level ($p = m$), Compute $\mathcal{R}_p^{ADER}$ and $\mathcal{R}_{P-1}^{ADER}$ at time level 0, also $\tau_0 = 0$
- Compute $\tau_1 = [\mathcal{R}_{p=m}^{ADER} - \mathcal{R}_{p-1}^{ADER}]|_0$
- Advance to time-level 1 by updating the state variable

$$\frac{dU}{dt} = \mathcal{R}_{p=m}^{ADER} + \tau_0$$

- At time-level 1, $p = m - 1$. Compute $\mathcal{R}_{p=m-1}^{ADER}$ and $\mathcal{R}_{P-1}^{ADER}$
- Compute $\tau_2 = [\mathcal{R}_{p=m-1}^{ADER} - \mathcal{R}_{p-1}^{ADER}]|_1 + \tau_1$
- Advance to time-level 2 by updating state variable solving

$$\frac{dU}{dt} = \mathcal{R}_{p=m-1}^{ADER} + \tau_1$$

- Continue recursively till the lowest order
- At the lowest order, $p = 1$,
  - Continue adding τ_m at the lowest level for required number of frozen time-steps (ν). Note that for a sawtooth cycle, $\nu = 1$.
  - Return to the highest-order accurate operator
- This finishes 1 ML cycle. Continue the process for N cycles.

Fig.2 shows the ML method in a saw-tooth form, in which a single time step is executed at all levels of approximation. Transition from the lowest order (1) to the highest order (m) does not require the forcing function to be added.

3 Results and Discussion

3.1 Numerical Accuracy

Grid convergence for ADER					
Order	Cells	L_1 error	L_1 order	L_∞ error	L_∞ order
2	25	5.11E-02	-	1.16E-01	-
	50	1.61E-02	1.67	4.94E-02	1.23
	100	4.72E-03	1.76	2.04E-02	1.27
	200	1.27E-03	1.89	8.36E-03	1.29
3	25	2.62E-03	-	4.46E-03	-
	50	3.30E-04	2.99	5.46E-04	3.03
	100	4.13E-05	3.00	6.60E-05	3.05
	200	5.16E-06	3.00	9.29E-06	2.83
4	25	6.52E-04	-	1.94E-03	-
	50	4.77E-05	3.77	2.07E-04	3.23
	100	3.34E-06	3.83	2.44E-05	3.08
	200	2.25E-07	3.89	2.66E-06	3.20

Table 1: Grid convergence study for the ADER scheme using ENO reconstruction

Grid convergence for ML-ADER					
Order	Cells	L_1 error	L_1 order	L_∞ error	L_∞ order
2	25	5.11E-02	-	1.16E-01	-
	50	1.61E-02	1.67	4.94E-02	1.23
	100	4.73E-03	1.77	2.04E-02	1.27
	200	1.28E-03	1.89	8.36E-03	1.29
3	25	2.63E-03	-	4.29E-03	-
	50	3.30E-04	2.99	5.86E-04	2.87
	100	4.13E-05	3.00	8.99E-05	2.71
	200	5.17E-06	3.00	1.18E-05	2.93
4	25	6.51E-04	-	1.93E-03	-
	50	4.78E-05	3.77	2.05E-04	3.24
	100	3.34E-06	3.84	2.45E-05	3.06
	200	2.28E-07	3.88	2.65E-06	3.21

Table 2: Grid convergence study for the ML-ADER scheme using ENO reconstruction

It can be analytically shown that the ML method retains high-order accuracy of the solution [4]. In order to test the numerical accuracy of the scheme, the scalar linear advection equation

$$u_t + au_x = 0, \qquad a = 1$$

is solved on 1D domain $[-1, 1]$ with periodic boundaries using ADER and the ML-ADER methods. A sine distribution $u(x, 0) = sin(\pi x)$ is used as the initial condition. The wave speed a is taken as unity. In both the cases, the simulation is run for time $t = 1$ units. ENO reconstruction is used for both ADER and ML-ADER flux computation. In both ADER and ML-ADER simulations, timestep is kept sufficiently small so that effect of timestepping is negligible.

L_1-errors and corresponding L_1-orders for the traditional ADER method are presented here in table 1. In table 2, L_1 errors and corresponding orders for ML-ADER method are shown. It can be seen, that the numerical accuracy of ML-ADER method is comparable to that of traditional ADER scheme.

3.2 Application to CAA

In this paper, two problems from computational aeroacoustics are solved using the ML-ADER method. The first problem [13] deals with propagation of acoustic waves in the upstream direction though a near-transonic convergent-divergent nozzle.

The quasi-1D nozzle is described with the following area distribution,

$$A(x) = \begin{cases} 0.536572 - 0.198086\ e^{-ln(2)\left(\frac{x}{0.6}\right)^2} & , \quad x > 0, \\ 1 - 0.661514\ e^{-ln(2)\left(\frac{x}{0.6}\right)^2} & , \quad x < 0 \end{cases} \tag{8}$$

Where, $x \in [-10, 10]$.

In order to simulate the acoustic wave propagation, linearized Euler equations in 1D are solved.

$$\mathbf{U}_t + \mathbf{A}\mathbf{U}_x = S \tag{9}$$

Where, $\mathbf{U}$ is the vector of the acoustic perturbations and $\mathbf{A}$ is the coefficient matrix based on the background flow in the nozzle, given as,

$$\mathbf{U} = \begin{bmatrix} \rho \\ u \\ p \end{bmatrix}, \ \mathbf{A} = \begin{bmatrix} u_0 & \rho_0 & 0 \\ 0 & u_0 & \frac{1}{\rho_0} \\ 0 & \gamma p_0 & u_0 \end{bmatrix} \tag{10}$$

ρ, u and p are density, velocity and pressure perturbation-variables respectively. The steady state values of

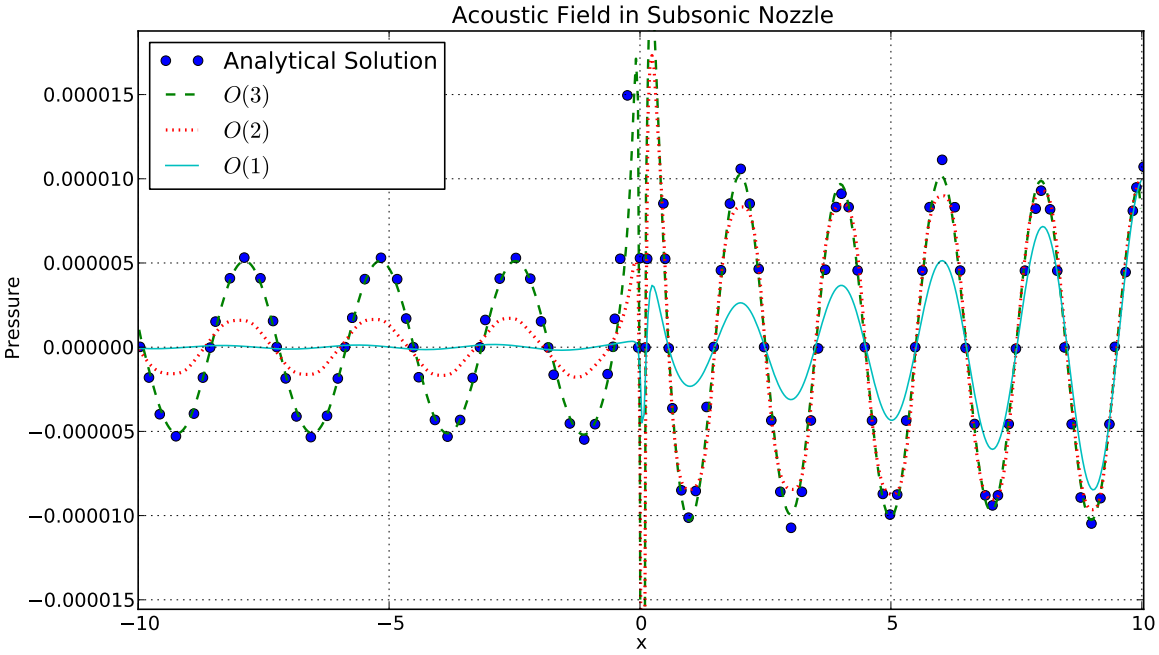

Figure 3: Acoustic waves travelling in upstream direction in a subsonic nozzle: Comparison of different spatial orders of accuracy

velocity(u_0), density(ρ_0) and pressure(p_0) correspond to steady state flow through a converging-diverging nozzle. These values can be found out either analytically or numerically. Analytical expressions for obtaining steady-state values are given in Ref.[13]. The steady state value of Mach number at exit of the nozzle is 0.4. A pulsating acoustic source is situated at the nozzle exit. The source term is given as,

$$\begin{bmatrix} \rho \\ u \\ p \end{bmatrix}_{acoustic} = 10^{-5} \begin{bmatrix} 1 \\ -1 \\ 1 \end{bmatrix} cos\left[\omega(\frac{x}{1-M}+t)\right] \tag{11}$$

As the flow in the nozzle is subsonic, acoustic waves travel in the upstream direction through the nozzle. For computing the acoustic waves, the system of equations(9) is first decoupled into characteristic variables. This is followed by higher-order reconstruction of state-variables and derivatives which in turn are used for ADER flux computations. Fig.3 shows acoustic pressure field computed with single-level ADER methods of different spatial orders. For these computations, the 1D domain is divided into 501 equi-spaced FV cells. It is clear from the figure, that higher order methods result in superior resolution of waves. Fig.4 shows comparison of acoustic pressure field computed with conventional and multi-level ADER methods. Results are obtained with saw-tooth and frozen-τ variants of ML-ADER method. A good agreement is seen between single-level and multi-level results.

In the second example [14], acoustic scattering from a 2D circular cylinder is simulated using conventional and multi-level ADER methods. For this simulation, a 2D system of linearized Euler equations is solved.

$$\mathbf{U}_t + \mathbf{A}\mathbf{U}_x + \mathbf{B}\mathbf{U}_y = 0 \tag{12}$$

Where, $\mathbf{U}$ is the vector of the acoustic perturbations and $\mathbf{A}, \mathbf{B}$ are the coefficient matrices, given as,

$$\mathbf{U} = \begin{bmatrix} p \\ u \\ v \end{bmatrix}, \ \mathbf{A} = \begin{bmatrix} u_0 & \rho_0 c_0^2 & 0 \\ \frac{1}{\rho_0} & u_0 & 0 \\ 0 & 0 & u_0 \end{bmatrix}, \ \mathbf{B} = \begin{bmatrix} v_0 & 0 & \rho_0 c_0^2 \\ 0 & v_0 & 0 \\ \frac{1}{\rho_0} & 0 & v_0 \end{bmatrix} \tag{13}$$

where, u, v are velocity-perturbation components in x and y direction and p is the pressure perturbation

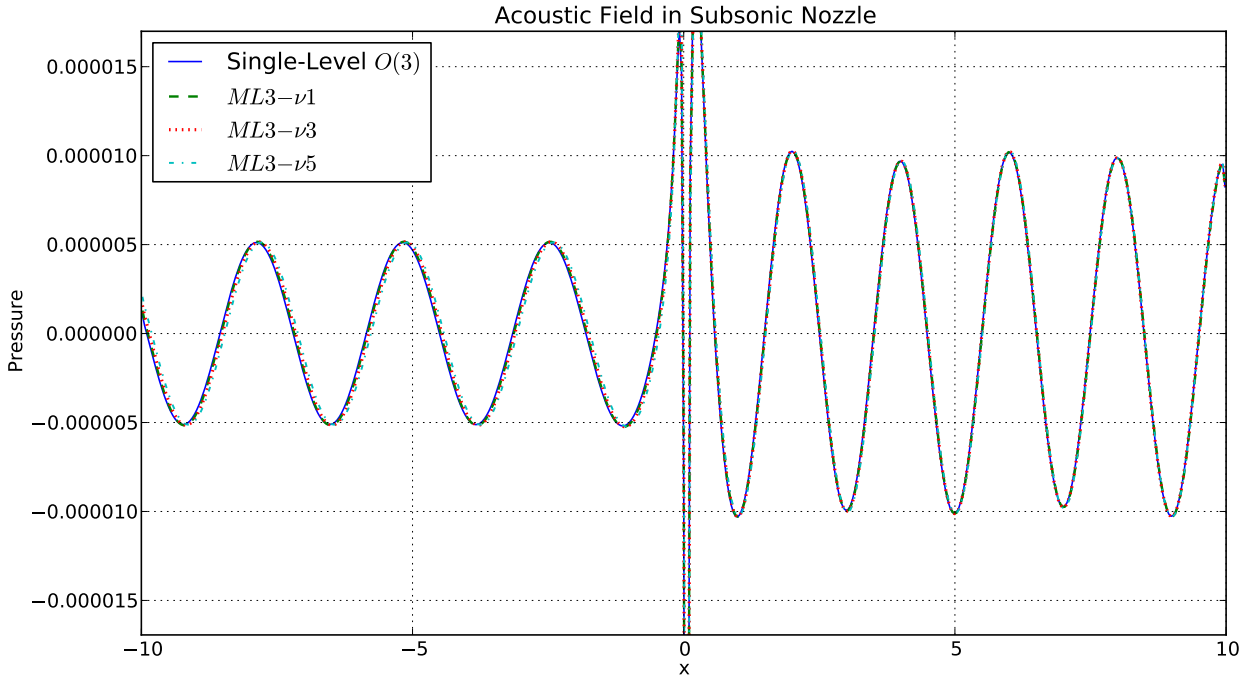

Figure 4: Acoustic waves travelling in upstream direction in a subsonic nozzle: Comparison of conventional and multilevel 3^{rd}-order ADER methods

variable. Initially (at $t = 0$) $u = v = 0$ and

$$p = exp\left[-ln2\left(\frac{(x-4)^2 + y^2}{(0.2)^2}\right)\right] \tag{14}$$

Also, the background velocity, $u_0 = v_0 = 0$.

At $t > 0$, an acoustic wave originating at $x = (4, 0)$ propagates in all directions. This wave reflects from a circular cylinder of radius 0.5 units situated at $(x, y) = (0, 0)$. Perturbation pressure at a point in the far-field (at $r = 5$, $\theta = 90^0$) is recorded at regular time intervals.

For this simulation, an axisymmetric grid consisting of 401 cells in θ direction and 201 cells in radial direction is used. Moreover, only half of the domain is considered because of the geometrical symmetry of the problem.

Fig.4 shows pressure history at a point $A(r = 5, \theta = 90^0)$ in far-field. Contour plot of pressure perturbations are shown in Fig.6. It can be seen that, the results obtained with ML-ADER method (and frozen τ variants) agree very well with the results from a conventional ADER method.

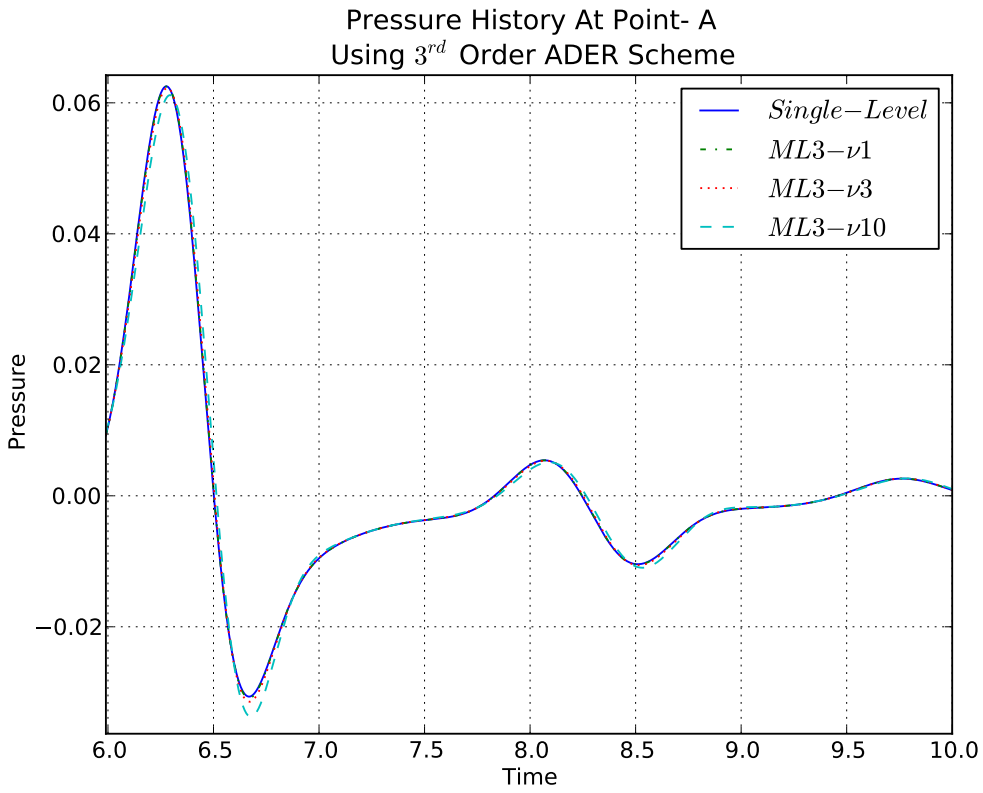

Figure 5: Comparison of the conventional and multilevel ADER methods: Pressure history at a point in far-field due to acoustic scattering from a 2D cylinder

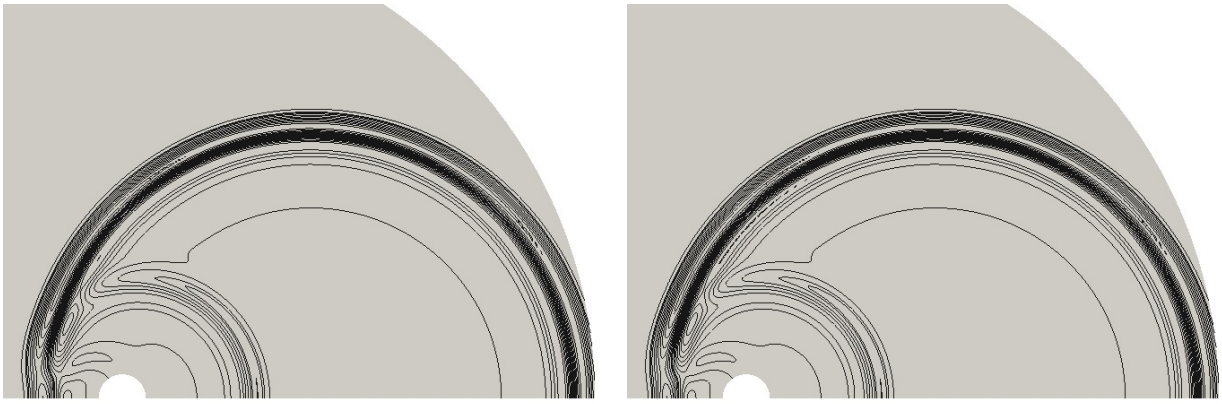

Figure 6: Acoustic scattering from a 2D circular cylinder: A. Contour plot with traditional ADER scheme B. Contour plot with ML-ADER method with $\nu = 1$

3.3 Computational Efficiency

Theoretically, the multilevel algorithm results in fraction of the computing cost as that of the single-level method of the same spatial order [4]. Table 3 shows computing time (in seconds) for simulating linear travelling waves using a scalar linear advection equation with single as well as multi-level methods. ENO

Computational Performance							
Order / Levels	Number of FV cells	CPU Time (S)		Normalized CPU Time (WU)		% Saving	Average Saving (%)
		ADER	ML-ADER	ADER	ML-ADER		
2	50	0.33	0.16	1.00E+00	4.85E - 01	46.59	
	100	1.31	0.68	3.97E+00	2.06E+00	47.95	
	200	6.79	3.56	2.06E+01	1.08E+01	47.57	47.92
	400	32.65	16.85	9.89E+01	5.11E+01	48.37	
	800	203.63	103.64	6.17E+02	3.14E+02	49.10	
3	50	1.06	0.47	1.00E+00	4.43E - 01	55.03	
	100	4.6	2.02	4.34E+00	1.91E+00	56.08	
	200	25.04	10.81	2.36E+01	1.02E+01	56.85	56.60
	400	123.66	53.25	1.17E+02	5.02E+01	56.93	
	800	805.82	337.57	7.60E+02	3.18E+02	58.10	
4	50	2.52	0.95	1.00E+00	3.77E - 01	62.35	
	100	11.15	4.23	4.42E+00	1.68E+00	62.08	
	200	59.82	23.13	2.37E+01	9.18E+00	61.32	62.27
	400	320.95	119.34	1.27E+02	4.74E+01	62.82	
	800	2112.37	786.29	8.38E+02	3.12E+02	62.77	

Table 3: Saving in computing time with two-level and three-level algorithms

reconstruction procedure is used in all simulations. All simulations are performed on Intel $i5-2500$ CPU (3.30GHz) running Linux.

In order to compare the computational performance of ML-ADER algorithm, computing time has been normalized with the time taken by ADER method on coarsest grid. As number of cells on domain are increased, Work Units(WU) required for both ADER and ML-ADER increase. However, WU required for ML-ADER are significantly less than WU for conventional ADER method. It can be seen that, ML-ADER method results in significantly reduced computing cost as compared to traditional ADER methods.

4 Conclusion

In this paper, a multilevel framework for the versatile ADER method is presented. The ML-ADER method is found to achieve higher-order accuracy at much lower computational cost. The method is found to be suitable for problems in computational aeroacoustics. The ML-ADER method does not require restriction and prolongation operators and can be blended with the existing finite volume framework.

References

[1] Schwartzkopff T. Munz C. D. and Toro E. F. ADER: A High-Order Approach for Linear Hyperbolic Systems in 2D. *Journal of Scientific Computing*, 17(1-4):231–240, 2002.

[2] Cunha G. and Redonnet S. On the Effective Accuracy of Spectral-Like Optimized Finite-Difference Schemes for Computational Aeroacoustics. *Journal of Computational Physics*, 263:222–232, apr 2014.

[3] Brandt A. Multi-level Adaptive Solutions to Boundary-Value Problems. *Mathematics of computation*, 31(138):333–390, 1977.

[4] Chatterjee A. A Multilevel Numerical Approach with Application in Time-Domain Electromagnetics. *Communications in Computational Physics*, 17(03):703–720, 2015.

[5] Chatterjee A. and Joshi S. M. Multilevel Higher Order Method for Simulation of Linear Wave Propagation. In *The Eighth International Conference on Computational Fluid Dynamics (ICCFD8)*, Chengdu, China, 2014.

[6] Toro E. F. Millington R. C. and Nejad L. A. M. Primitive Upwind Numerical Methods for Hyper-

bolic Partial Differential Equations. In C. H. Bruneau, editor, *Sixteenth International Conference on Numerical Methods in Fluid Dynamics. Lecture Notes in Physics*, pages 421–426. Springer-Verlag, 1998.

[7] Ben-Artzi M. and Falcovitz J. A Second-Order Godunov-Type Scheme for Compressible Fluid Dynamics. *Journal of Computational Physics*, 1984.

[8] Schwartzkopff T. Dumbser M. and Munz C. D. Fast High Order ADER Schemes for Linear Hyperbolic Equations. *Journal of Computational Physics*, 197(2):532–539, 2004.

[9] Titarev V. and Toro E. F. ADER: Arbitrary High Order Godunov Approach. *Journal of Scientific Computing*, 17(1-4):609–618, 2002.

[10] Toro E. F. and Titarev V. a. ADER Schemes for Scalar Non-Linear Hyperbolic Conservation Laws With Source Terms in Three-Space Dimensions. *Journal of Computational Physics*, 202(1):196–215, 2005.

[11] Titarev V. a. and Toro E. F. ADER Schemes for Three-Dimensional Non-Linear Hyperbolic Systems. *Journal of Computational Physics*, 204(2):715–736, 2005.

[12] Toro E. F. and Titarev V. Derivative Riemann Solvers for Systems of Conservation Laws and ADER Methods. *Journal of Computational Physics*, 212(1):150–165, 2006.

[13] Tam C. K. W. and Webb J. C. Third Computational Aeroacoustics (CAA) Workshop on Benchmark Problems. 2004.

[14] Tam C. K. W. and Hardin J. C. Second Computational Aeroacoustics(CAA) Workshop on Benchmark Problems. 1997.